

SO₂ and BrO observation in the plume of the Eyjafjallajökull volcano 2010: CARIBIC and GOME-2 retrievals

K.-P. Heue¹, C. A. M. Brenninkmeijer¹, A. K. Baker¹, A. Rauthe-Schöch¹, D. Walter^{1,3}, T. Wagner¹, C. Hörmann^{1,3}, H. Sihler^{1,3}, B. Dix², U. Frieß³, U. Platt³, B. G. Martinsson⁴, P. F. J. van Velthoven⁵, A. Zahn⁶, and R. Ebinghaus⁷

¹Max-Planck-Institut für Chemie (MPI), Mainz, Germany

²Department of Chemistry and Biochemistry, University of Colorado, Boulder, CO, USA

³Institut für Umweltp Physik, Universität Heidelberg, Heidelberg, Germany

⁴Avdelningen för kärnfysik, Lunds universitet, Lund, Sweden

⁵Koninklijk Nederlands Meteorologisch Instituut (KNMI), De Bilt, The Netherlands

⁶Institut für Meteorologie und Klimaforschung (IMK), Karlsruher Institut für Technologie (KIT), Karlsruhe, Germany

⁷Institut für Küstenforschung, GKSS, Geesthacht, Germany

Received: 20 October 2010 – Published in Atmos. Chem. Phys. Discuss.: 6 December 2010

Revised: 22 February 2011 – Accepted: 24 March 2011 – Published: 31 March 2011

Abstract. The ash cloud of the Eyjafjallajökull (also referred to as: Eyjafjalla (e.g. Schumann et al., 2011), Eyjafjöll or Eyjafjöll (e.g. Ansmann et al., 2010)) volcano on Iceland caused closure of large parts of European airspace in April and May 2010. For the validation and improvement of the European volcanic ash forecast models several research flights were performed. Also the CARIBIC (Civil Aircraft for the Regular Investigation of the atmosphere Based on an Instrument Container) flying laboratory, which routinely measures at cruise altitude (≈ 11 km) performed three dedicated measurements flights through sections of the ash plume. Although the focus of these flights was on the detection and quantification of the volcanic ash, we report here on sulphur dioxide (SO₂) and bromine monoxide (BrO) measurements with the CARIBIC DOAS (Differential Optical Absorption Spectroscopy) instrument during the second of these special flights on 16 May 2010. As the BrO and the SO₂ observations coincide, we assume the BrO to have been formed inside the volcanic plume. Average SO₂ and BrO mixing ratios of ≈ 40 ppb and ≈ 5 ppt respectively are retrieved inside the plume. The BrO to SO₂ ratio retrieved from the CARIBIC observation is $\approx 1.3 \times 10^{-4}$. Both SO₂ and BrO observations agree well with simultaneous satellite (GOME-2) observations. SO₂ column densities retrieved from satellite observations are often used as an indicator for volcanic ash. As the CARIBIC O₄ column densities changed rapidly during the

plume observation, we conclude that the aerosol and the SO₂ plume are collocated. For SO₂ some additional information on the local distribution can be derived from a comparison of forward and back scan GOME-2 data. More details on the local plume size and position are retrieved by combining CARIBIC and GOME-2 data.

1 Introduction

Volcanic eruptions emit large amounts of ash and reactive gases into the atmosphere. Depending on the mass and altitude of ashes emitted, the geographical position of the volcano and the local meteorological conditions, the influence on atmospheric composition varies between local and global (e.g. Pinatubo 1991). As an explosive eruption of the Icelandic volcano Eyjafjallajökull (63° 37' 48" N 19° 37' 12" W) from 14 April to 24 May 2010 demonstrated, a modest volcanic eruption can have serious atmospheric consequences as large parts of the western European airspace were closed. Satellite observations of Eyjafjallajökull's plume showed enhanced values of sulphur dioxide (SO₂) mainly after 19 April 2010. Sulphur dioxide is often used as tracer for volcanic plumes and hence for volcanic ash (Carn et al., 2009). Moreover, volcanic bromine monoxide (BrO) was detected by satellite measurements close to Iceland but also further downwind, suggesting that bromine was emitted by the Eyjafjallajökull as well.

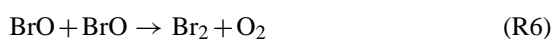
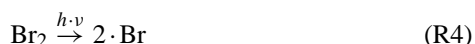
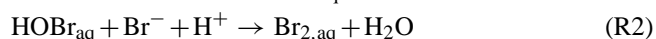


Correspondence to: K.-P. Heue
(klaus-peter.heue@mpic.de)

Here we present observations of SO₂ and BrO north of Ireland on 16 May 2010. Based on the combination of the DOAS CARIBIC data with GOME-2 satellite data additional information on spatial distribution details can be gained. The data were recorded during a special mission of the CARIBIC observatory (Civil Aircraft for the Regular Investigation of the atmosphere Based on an Instrument Container, <http://www.caribic.de/>, Brenninkmeijer et al., 2007) deployed on board of a Lufthansa Airbus A340-600 passenger aeroplane. Three special flights were aimed at a fairly complete observation of the volcanic plume by means of in situ trace gas and aerosol measurements, complemented by air and aerosol sampling. As the SO₂ and BrO column densities were below the detection limit during the first flight (20 April 2010, when the plume originated from the first eruption phase having low SO₂ emissions), and the DOAS instrument malfunctioned during the third (19 May 2010), we focus on the second flight. Besides the Lufthansa CARIBIC measurement flights, other airborne measurements (e.g. Schumann et al., 2011) as well as ground based observations of the plume by lidar and ozone soundings were made (e.g. Ansmann et al., 2010; Flentje et al., 2010).

The chemical processes inside volcanic plumes have been studied for a considerable time. Since Bobrowski et al. (2003) detected large amounts of BrO downwind of the Soufrière Hills volcano (Montserrat) measurements (and simulation studies) also target the chemistry of halogen compounds. A few years later volcanic BrO emissions were also studied using aircraft measurements (Bani et al., 2009) and satellite observations (Theys et al., 2009). Compared to ground based measurements both airborne and satellite observation offer the advantage that measurements at various distances from the crater can be performed with the same instrument. While satellites often have a coarse spatial resolution compared to aircraft observations, they can follow the plume over long distances (e.g. from Iceland to the British Isles).

An overview of the chemistry in the plumes of degassing volcanoes is given by von Glasow et al. (2009). While sulphur dioxide (SO₂) is directly emitted by volcanoes, bromine monoxide (BrO) forms inside their plumes primarily through heterogeneous reactions. The mechanism is similar to the one observed in polar spring leading to the “bromine explosion” and the concurrent arctic tropospheric ozone depletion events (e.g. Simpson et al., 2007). The main chemical reactions are shown below:



Hence the production of BrO takes only place under daylight conditions (Eq. R4). Moreover the mixing ratio of ozone must be maintained at a sufficient level through mixing-in of background air from outside the plume. Other studies (Bobrowski et al., 2007) on volcanic BrO close to a crater observed a higher BrO concentration towards the plume edges compared to the centre. They concluded that the enhanced mixing in of ozone towards the edges caused the higher BrO concentration there, in contrast to the plume centre, where the ozone concentration is too low.

Instead of Br₂ also BrX (X = F, Cl or I) may be released from the aerosols and become photo dissociated, leading to a small halogen source. Indeed chlorine oxides (ClO, OClO) have been observed in volcanic plumes (e.g. Bobrowski et al., 2007). For the CARIBIC flight we report here, evidence for the presence of chlorine radicals will be presented elsewhere (Baker et al., 2011).

2 Description of the instruments

2.1 CARIBIC project

CARIBIC is based on a Lufthansa Airbus A340-600 retrofitted with a three probe (trace gases, water and aerosol) inlet system. Under normal operations the aeroplane carries the instrument container on a monthly basis during four consecutive regular passenger flights for 2–4 days. CO, CO₂, O₃, NO, NO₂, NO_y, CH₄, some organic compounds (e.g. acetone), mercury, total and gaseous water and aerosols are measured in real time. In addition, 16 aerosol samples and 116 air samples (28 prior to spring 2010) are collected for post flight laboratory analysis of aerosol elemental composition, (Nguyen et al., 2006) and of a host of trace gases (Schuck et al., 2009; Baker et al., 2010). A video camera in the inlet pylon takes a frame every second for post flight cloud cover analysis. Furthermore three miniature DOAS telescopes are mounted in the pylon. The instruments are maintained and operated by nine scientific groups from institutes in Europe (<http://www.caribic-atmospheric.com/>, January 2011).

The instrumental container was updated in winter 2009/2010 with three new instruments: a new high resolution air sampler for 88 additional air samples, a cavity ring down absorption spectrometer (CRDS) for the D/H and ¹⁸O/¹⁶O ratios of water (Dyroff et al., 2010) and an off-axis integrated cavity output spectrometer (OA-ICOS) for in situ measurements of CH₄ and CO₂ (Kattner et al., 2010). A new optical particle counter (OPC) for the aerosol size distribution between 125 nm and 1 μm replaced an older one. The O₃ analyser and the H₂O instruments were improved while the NO_y instrument was extended for NO₂. Also the DOAS instrument was completely upgraded (Sect. 2.3).

The trace gas and aerosol measurements are complemented by standard in flight observations from the aeroplane (e.g. position, temperature, wind speed, pressure) which are

Table 1. DOAS retrieval settings for the CARIBIC and GOME-2 data retrieval.

Wavelength Range [nm]	CARIBIC			GOME-2	
	SO ₂	BrO	O ₄	SO ₂	BrO
	311.6–333	324–354	332–367	312.1–324	336–360
O ₃	Bogumil et al. (2003, 223 K and 243 K)			Gür et al. (2005, 223 K and 243 K)	
NO ₂	Vandaele et al. (1996)			–	Vandaele et al. (1996)
BrO	Wilmouth et al. (1999, 228 K)			–	Wilmouth et al. (1999, 228 K)
SO ₂	Bogumil et al. (2003, 273 K)	–	–	Bogumil et al. (2003, 273 K)	
O ₄	–	Greenblatt et al. (1990)	–	Greenblatt et al. (1990)	
OCIO	Kromminga et al. (2003)			–	Bogumil et al. (2003)
HCHO	–	Meller and Moortgat (2000)	–	Bogumil et al. (2003)	
Polynomial degree	4	5	5	4	4

provided by Lufthansa. The Royal Dutch Meteorological Institute (KNMI) supports the CARIBIC project with trajectory calculations along the flight track based on the TRAJKS model (Scheele et al., 1996; Stohl et al., 2001). Both forward and backward trajectories for 2 and 8 days respectively are calculated using ECMWF weather data interpolated to the position and time of the CARIBIC observation.

2.2 The DOAS technique

The DOAS instruments (Sects. 2.3 and 2.4) measure scattered sunlight and Differential Optical Absorption Spectroscopy (DOAS) (Platt and Stutz, 2008) is used to retrieve information about trace gas amounts in the atmosphere. DOAS is based on the Lambert-Beer law:

$$I(\lambda) = I_0(\lambda) \cdot e^{-\text{SCD} \cdot \sigma(\lambda)} \quad (1)$$

It describes the reduction in the intensity I_0 at a certain wavelength (λ) when passing through a medium with absorption cross section ($\sigma(\lambda)$), with SCD (slant column density) being the absorber concentration (c) integrated along the light path:

$$\text{SCD} = \int_{\text{lightpath}} c(\mathbf{r}) \cdot d\mathbf{r} \quad (2)$$

Since many atmospheric trace gases e.g. NO₂, SO₂, BrO, O₃, O₄ or HCHO have unique absorption cross sections in the UV/Vis wavelength range, several tracers can be quantified simultaneously when using a certain wavelength interval. In principle the determination of SCDs requires knowledge of the solar radiation I_0 before entering the atmosphere. However, as this cannot be measured with the same instrument and the strong Fraunhofer absorptions have to be removed, a reference spectrum is included in the retrieval. By including a reference spectrum the absorption of the reference relative to the solar radiation is subtracted in the retrieval. Because of

that the retrieved slant column is a differential column, relative to the reference spectrum. In this study we used as reference a cloudy spectrum recorded shortly after crossing the plume (10:35 UTC), assuming that the cloud coverage and cloud optical density were similar to those below the plume. For some trace gases, e.g. BrO, the subtraction of the reference spectrum automatically includes the correction for the stratospheric signal, if the change in the solar zenith angle is small enough. Table 1 shows an overview of the settings used for DOAS data analysis of both the CARIBIC and the GOME-2 spectra.

The filling-in of the Fraunhofer lines caused by inelastic scattering of light (Grainger and Ring, 1962) was corrected by including a Ring spectrum (Bussemer, 1993; Wagner et al., 2009) in the retrieval. The Ring spectrum is calculated from the reference or a direct sunlight spectrum for GOME-2. In Table 1 OCIO and HCHO are also listed for the CARIBIC DOAS retrieval, however these two trace gases were found to be below the detection limit of 6×10^{13} molec/cm² and 1.5×10^{16} molec/cm², respectively. Based on the detection limit a maximum concentration of ≈ 4 ppt for OCIO and 1 ppb for HCHO can be estimated in the plume as described below (Sect. 4.1).

In Fig. 1 an example fit for the CARIBIC DOAS data for the three wavelength ranges is shown (nadir, 9 spectra co added and 1 omitted). Only a few trace gas absorptions are depicted here to keep the figure clear. On top SO₂ and O₄ fits are shown for the respective wavelength interval, in the centre the BrO fit is shown and in the lowest row the residuals for all wavelength intervals are given. There are small structures in the SO₂ residual, caused by an imperfect O₃ fit. However as the SO₂ absorptions are strong, these structures do not affect the observed SO₂ SCD. The observed O₄ column densities in the nadir spectra are small. For consistency the CARIBIC DOAS spectra were also analysed in the same wavelength intervals as the GOME-2 spectra. The differences between the two retrieval settings were found to be

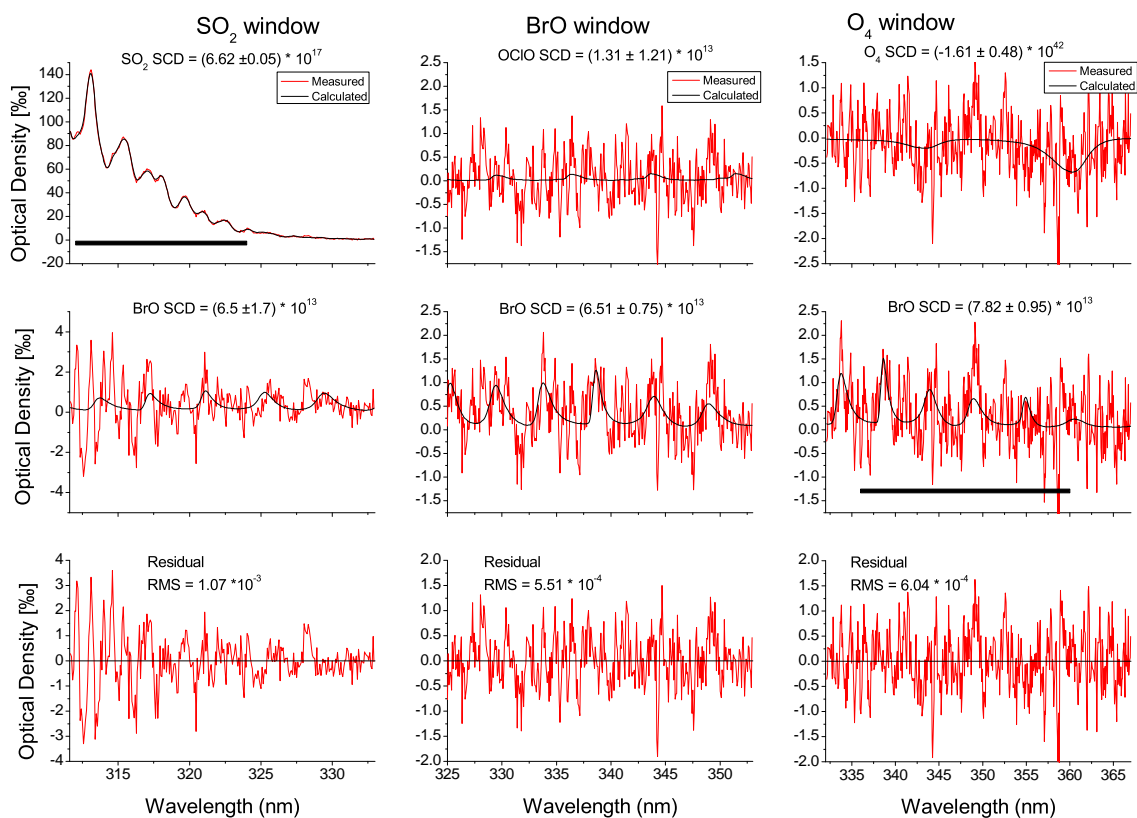


Fig. 1. Example fit for the three different wavelength intervals (shown in the three columns) for spectrum C4000160 (9 spectra co-added, 1 omitted 10:19:28–10:20:50 UT) of the nadir spectrometer (6.66° W, 56.14° N, 4580 m a.s.l. – inside the plume). The black bars in the SO₂ and O₄ windows show the SO₂ and BrO fit window used in the GOME-2 retrieval (Table 1).

within their errors. Also the BrO fit interval was extended towards shorter wavelengths, to check for the influence of the imperfect O₃ fit (Fig. 1 SO₂ window). Until ≈ 320 nm no significant change in the BrO SCDs was observed.

As the slant column density is highly dependent on factors like viewing geometry, solar position, altitude profile of the trace gas, cloud coverage and aerosol content (Sect. 3.2), the vertical column density is introduced to compare the observation with other data e.g. satellite observations. The vertical column density (VCD) is defined as the height integral of the concentration:

$$\text{VCD} = \int_0^{\text{TOA}} c(z) \cdot dz \quad (3)$$

$$\text{AMF} = \frac{\text{SCD}}{\text{VCD}} \quad (4)$$

For the conversion of measured SCD to VCD an Air Mass Factor (AMF) is introduced as the ratio between SCD and VCD (Eq. 4). The AMF is numerically simulated under consideration of all above mentioned parameters. We used the radiative transfer model McArtim (Deutschmann, 2009), which is a full spherical Monte Carlo radiative transfer model, to retrieve the AMFs. Because of the Monte Carlo

algorithm, the AMF has a statistical error. Together with the simulated AMF the 1σ variance is estimated by the program. For our study the statistical error in the AMFs is below 7%. The error caused by wrong assumptions concerning cloud cover, plume altitude, aerosols and other parameters can be much higher, therefore in Sect. 3.2 the best estimates for these parameter are discussed.

The typical fit error for BrO for 10 co-added CARIBIC spectra was around 1×10^{13} molec/cm², which is similar or slightly higher than depicted in Fig. 1. For SO₂ the error in the SCD is in most cases less than 4×10^{15} molec/cm² for the averaged nadir data. Due to the low optical density of BrO the relative measurement errors are higher. For the individual spectra the typical errors for both slant and vertical columns are listed in Table 2, for a better comparison the errors of the GOME-2 retrieval are included.

2.3 DOAS on CARIBIC

The CARIBIC DOAS instrument is described in detail in Dix et al. (2009) and Heue et al. (2010). It observes scattered sunlight under three different elevation angles (-82° named nadir, -10° , and $+10^\circ$ relative to the horizon). The three small telescopes (opening angle = 1.9°) present in the

Table 2. Error estimates for BrO and SO₂ vertical column densities for an individual CARIBIC spectrum (-10° and nadir) and GOME-2 during the observation of the plume (Sect. 4.1).

	BrO			SO ₂		
	Δ AMF [%]	Δ SCD [10^{13} molec/cm ²]	Δ VCD	Δ AMF [%]	Δ SCD [10^{16} molec/cm ²]	Δ VCD
-10°	7	6	1.8	7	2	1.9
nadir	7	2	0.8	7	0.8	1.8
GOME-2	7	3	1.6	7	5	3.4

CARIBIC-pylon are connected to the three spectrometers mounted in the container via three quartz fibre bundles. In Winter 2009/2010 the existing Ocean Optic USB2000 spectrometers were replaced by new CTF60 spectrometers from OMT (Optische Messtechnik, Ulm, Germany). The wavelength ranges of all spectrometers cover the interval from 300 to 400 nm with a spectral resolution of 0.5 nm (full width at half maximum). Hence it allows us to retrieve sulphur dioxide from all 3 lines of sight, in contrast to the old DOAS system (Heue et al., 2010). Moreover the time resolution could be reduced from 30 to 8 s (corresponding to 7.5 km and 2 km horizontal resolution, respectively) without increasing the measurement errors.

Unfortunately during the same period the quartz fibres in the bundle connecting the $+10^\circ$ telescope with its spectrometer were damaged and could not be replaced before the volcanic flights. Hence, for this study, only two viewing directions were active. Moreover since these were the first data recorded with the new system (immediately after the recertification of the CARIBIC container following the upgrades) some parameter settings were still suboptimal. Particularly the intensity detected with the -10° spectrometer was far below that of nadir and some spectra reached oversaturation since the determination of the integration time had to be optimized under real flight conditions. Apart from the high temporal resolution analyses of all spectra, occasionally up to ten spectra were co-added (excluding the oversaturated ones) to reduce noise and improve the detection limit.

2.4 GOME-2 on MetOp-A

GOME-2 (Global Ozone Monitoring Experiment) is the first of a series of three identical instruments. Its platform, MetOp-A, was launched into a sun-synchronous polar orbit at 800 km altitude in October 2006 and crosses the equator at 09:30 LT (local time). The GOME-2 instrument is a 4 channel UV/Vis grating spectrometer, which covers the wavelength region of 240–790 nm with a spectral resolution of 0.2–0.4 nm. Besides the backscattered and reflected radiance from the Earth it also observes direct sunlight. The ground pixel size is roughly 80 x 40 km² and the total swath width is 1920 km (24 pixels wide), thereby achieving daily coverage at mid latitudes (<http://www.esa.int/esaLP/LPmetop>).

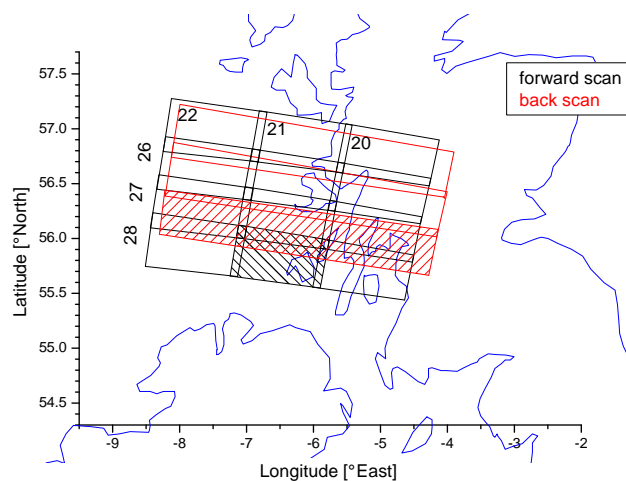


Fig. 2. Forward (black) and back scans (red) of the GOME-2 instrument north of Ireland (16 May 2010 10:09 UTC). For both scanning modes one pixel is hatched to emphasise the size of the individual pixels and to illustrate the overlapping areas. The numbers in the forward pixels indicate the pixel number, while the swath number is written to the left.

html, September 2009). The respective pixels are scanned from the east to the west by rotating a mirror in the optical system of the entrance optics. When it turns back, the respective "back scan" pixel (240 x 40 km²) is obtained. The forward and backward scan pixel partially overlap (Figs. 2 and 14). In Fig. 2 1/8 of the total swath is shown, it has 24 forward and 8 back scan pixels. The figure can be extended to both sides, and so the back scans shown here also partly overlap with the previous forward scans to the east, which are not shown.

Details of the DOAS retrieval are listed in Table 1 and in Heue et al. (2010). For the SO₂ retrieval the O₃ cross section (223 K) was scaled with a 4th order polynomial, because Rayleigh scattering causes a systematic change of the atmospheric light paths within the selected fitting window (e.g. van Roozendaal et al., 2006; Pukite et al., 2010). It should be noted that in principle additional ozone absorption cross sections for higher temperatures might be included in the fitting algorithm (Table 1). However, for a similar case study, no significant change of the retrieved SO₂ results and the magnitude of the residual was found, if additional temperatures were considered (Heue et al., 2010).

The retrieval errors are included in Table 2. As a matter of fact, the retrieved BrO column densities in the plume ($\approx 6 \times 10^{13}$ molec/cm²) are close to the detection limit. Nevertheless the comparison with the CARIBIC columns shows quite good agreement (Sect. 4.2.2).

In order to calculate the vertical column density in the plume, the measured slant column densities were corrected for the latitudinal and longitudinal dependent offset, which in the case of SO₂ is mainly caused by the spectral interference

with ozone or imperfect fitting of the Ring effect. In the case of BrO, the observed volcanic signal is superimposed on the strongly latitudinal-dependent stratospheric BrO distribution. The correction process was only applied to a pre-selected area of interest (38° W–15° E, 35° N–72° N), including 3 adjacent GOME-2 orbits. To account for the different viewing directions of the individual pixel, the SO₂ and BrO SCDs are converted to VCD_{geom} by applying the geometric AMF:

$$\text{AMF}_{\text{geom}} = \frac{1}{\sin(-\text{LOS})} + \frac{1}{\cos(\text{SZA})} \quad (5)$$

Here, LOS and SZA are the line of sight (nadir = −90°) and the solar zenith angle, respectively. As the $\text{VCD}_{\text{geom}} = \frac{\text{SCD}}{\text{AMF}_{\text{geom}}}$ is independent of the LOS, the background can now be estimated as a smooth function of the pixels outside the plume. Therefore, a 2-dimensional 3rd order polynomial fit was applied to the VCD of all pixels, whose SO₂ VCD does not exceed the 2σ variation (and therefore are supposed not to be part of the volcanic plume).

The corresponding BrO VCDs_{geom} were fitted to the same background pixels using a 2-dimensional 4th order polynomial. By subtracting the resulting polynomial from all VCDs (including the VCDs from the presumed volcanic plume pixels) we obtained the offset corrected (normalised) vertical column densities VCD_{norm}. These data products were used for the overview plots (Fig. 9).

During the plume observation the SZA was ≈44°, hence the geometrical AMF varied between 2.4 (nadir) and 2.8 (LOS −135° and −45°). For the direct comparison to the CARIBIC DOAS observation (Sect. 4.2) radiative transfer simulations with McArtim (Sect. 2.2 Deutschmann, 2009) were performed including the same cloud and aerosol settings as for CARIBIC DOAS (Sect. 3.2). Beforehand the corrected VCD_{norm} is multiplied with the geometric AMF to calculate a corrected slant column density SCD_{norm}.

3 Observations

3.1 Measurement flights

Three special measurement flights were performed to help validate the volcanic ash forecasts. Several forecast models (e.g. Volcanic Ash Advisory Centre (VAAC), British Met Office (Fig. 3), Eurad (Universität Köln, Germany), Flexpart (Norsk Institutt for Luftforskning (NILU), Norway)) were compared to get the best possible estimate on the plume's position and movement. Obviously no-fly zones as stipulated by the VAAC London had to be avoided at all times. According to the forecasts (Fig. 3) for 16 May 2010 the optimal areas to observe particle mass concentrations close to the given aviation safety threshold of 2000 μg/m³ were over Ireland and the Irish Sea and accordingly these areas were

probed, with a first leg over Ireland and a second one over the Irish Sea.

The actual flight pattern is shown in Fig. 4 and 5. As the airspace north of the Isle of Man (≈54° N) was closed, the aeroplane had to turn south at this point. During the plume observation the flight altitude varied between 2 and 7 km. This altitude range was chosen because above flight level 200 (≈6 km) the models predicted low concentrations. On the same day the DLR Falcon also performed measurements over the British Isles and its lidar observed the maximum plume altitude at 7 km (Schumann et al., 2011) only a few hundred kilometres east over the North Sea close to the British coast (54.6° N, 0.2° W).

The TRAJKS back trajectories (http://www.knmi.nl/samenw/campaign_support/CARIBIC/, January 2011) calculated for various positions along the CARIBIC flight track indicate that the air masses showing the highest volcanic signals (Sect. 3.2 - north of Ireland) had passed over southern Iceland 34–53 h before the observation (Fig. 4).

3.2 CARIBIC DOAS observation

The DOAS instrument observed three major enhancements of SO₂ (Fig. 5). Two of these were very close together (10:05–10:25) and a third, weaker one was measured about 2 hours later over the Irish Sea. The first two SO₂ peaks can be attributed to the same plume (Fig. 5). It was observed north of Ireland (Fig. 5) just before and after the u-turn. At the same time enhanced BrO was observed as shown in Figures 1 and 5.

We are confident that the SO₂ third peak is just the edge of the large plume that extended further north (Fig. 9), although the CARIBIC aeroplane could not fly further north due to the aviation safety rules. At the plume's edge no BrO was observed. Based on the elemental composition of aerosol sample No 6 taken between 11:38 and 12:27 (Fig. 5), the minor peak south of the Isle of Man can also be attributed to the volcanic plume (Sect. 3.3.1).

The oxygen dimer O₄ provides a standard tool for passive DOAS observations to estimate the aerosol optical thickness along the light path (e.g. Wagner et al., 2004; Frieß et al., 2006; Heue, 2005). Therefore the observed O₄ slant column densities are compared to calculated SCDs (Sect. 2.3) based on radiative transfer simulations. The parametrisation of the aerosol extinction in the model is adapted to the measurement. Other parameters e.g. cloud cover (discussed below), solar zenith angle, and viewing geometry are included in the model. In Fig. 6 the decrease in the O₄ SCD and the simultaneous increase in the SO₂ column densities are shown. The coincidence with the SO₂ peaks indicates convincingly that volcanic aerosols caused the observed reductions in the light path.

Because there was nearly complete cloud cover below the aeroplane, the cloud top height and optical thickness have to be included in the radiative transfer simulation. The video

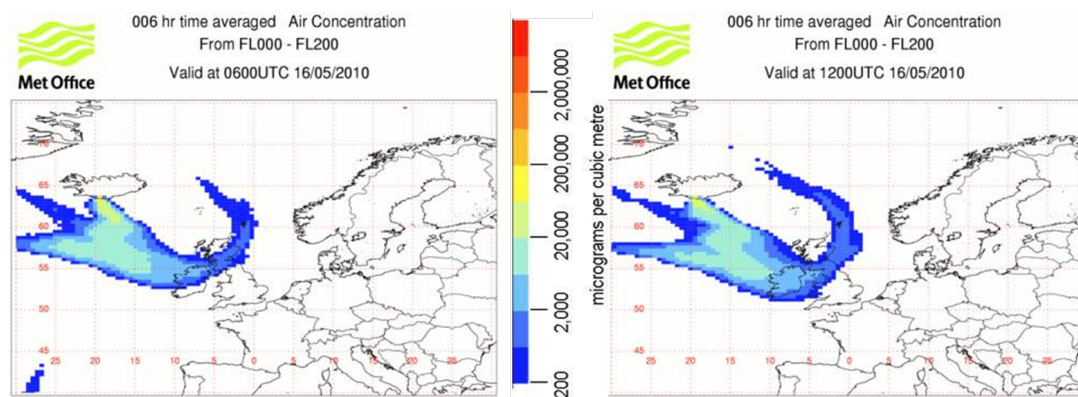


Fig. 3. The volcanic ash forecast from the British Met Office for 16 May 2010, 06:00 UTC (left) and 12:00 UTC (right) for the flight levels 0 to 200 (surface to 6.1 km). The centre of the plume was expected to be south of Iceland and expanding over Ireland with a small filament reaching from northern England almost back to Iceland. Comparing the two panels shows that the plume was expected to move south-east.

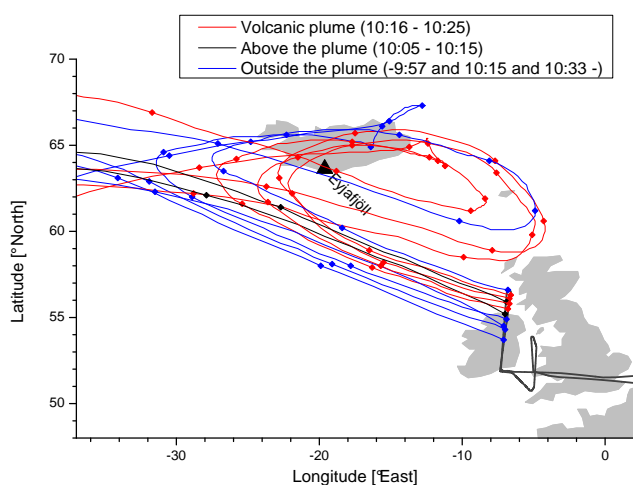


Fig. 4. TRAJKS backward trajectories, for the time of the CARIBIC plume observation. The dots along the trajectories label 12 hours intervals. With the DOAS the plume was observed twice, as the aeroplane crossed the plume and subsequently descended to the plume altitude (Sect. 3.2 and 3.3). The trajectories for the period during which many other instruments showed influence of volcanic air masses are illustrated in red, the blue lines show clean air, and the black lines stand for the periods of enhanced DOAS SO₂ signal without additional indicators for volcanic influences. The origin of the enhanced SO₂ values can be traced back to the Eyjafjallajökull volcano on Iceland, which the air masses had passed 34–53 hours before CARIBIC sampled the plume (16 May 2010 10:20 UTC).

camera in the pylon has an elevation of -13.2° and a field of view of 36° . When a cloud is first observed in the centre of the video image and a few seconds later at its lower edge, this information can be used to estimate the cloud top height ($1500 \text{ m} \pm 500 \text{ m}$). The low resolution of the video images however limits the accuracy of this method. Nevertheless the

results agree well with independent observations (MODIS – <http://ladsweb.nascom.nasa.gov/>, August 2010) of the cloud top height. Hence in the radiative transfer simulation the cloud top height was fixed to 1.5 km. The geometrical and optical thickness (COT) of the cloud were set to 1 km and 10 (Fig. 7), respectively. The horizontal variability in the COT seems to be small (Fig. 7), hence we assumed the same cloud parameters for the plume as well as for the reference.

The geometrical thickness of the plume was assumed to be constant, with its bottom at 3 and its top at 6 km altitude (U. Schumann, personal communication, 2010). For simulating the optical properties of the volcanic ash cloud, the aerosol optical thickness and the single scattering albedo were varied in the range from 0.3 km^{-1} to 2.5 km^{-1} and from 0.8 to 0.99, respectively. Figure 6 shows an example of the simulated O₄ column densities for three different values of the single scattering albedo (SSA). For the -10° telescope O₄ data a SSA between 0.95 and 0.99 would be best, however also the nadir data and the intensity of the spectra are considered for the aerosol retrieval. As the algorithm to calculate the exposure time of the spectrometers still had to be optimised, the intensity ratios were weighted by only 10% compared to the O₄ columns. An aerosol extinction of 0.8 km^{-1} combined with a single scattering albedo of 0.95 leads to the best agreement between simulations and observations. The retrieved SSA also agrees well with the values (0.96 at 330nm) retrieved from the OPC observations during the third CARIBIC volcano flight (19 May 2010). Compared to the MODIS observations the Aerosol Optical Thickness (AOT ≈ 1) is much higher, which can at least partly be explained with the higher spatial resolution of the CARIBIC DOAS instrument (2 km to 15 km) and the slight temporal mismatch (10:20 UTC for CARIBIC and 10:56 UTC for MODIS) combined with the strong variability of the volcanic ash cloud.

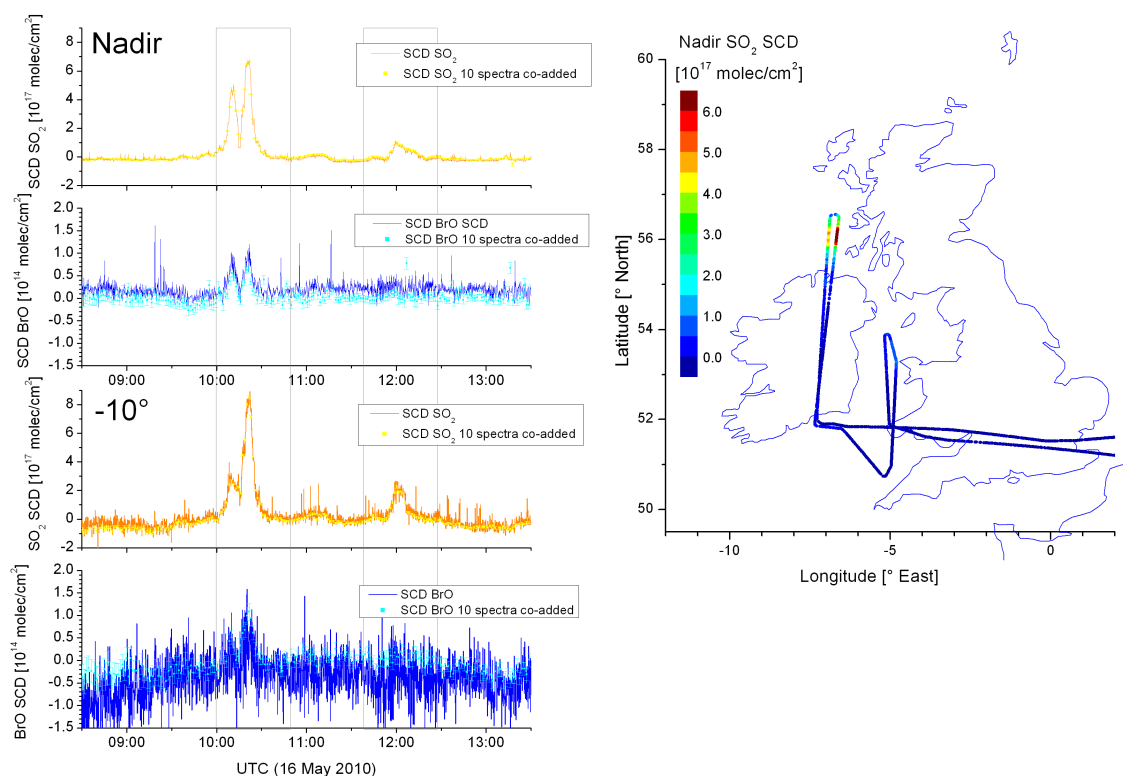


Fig. 5. Time series of the SO₂ and the BrO CARIBIC DOAS SCDs for nadir and -10° and the spatial SO₂ distribution (right) for nadir. The two strong enhancements can clearly be attributed to the same plume which was crossed twice just before and after the u-turn north of Ireland. The boxes indicate the two time intervals during which the collected aerosol samples showed clear evidence of volcanic ash (samples No 4 and No 6).

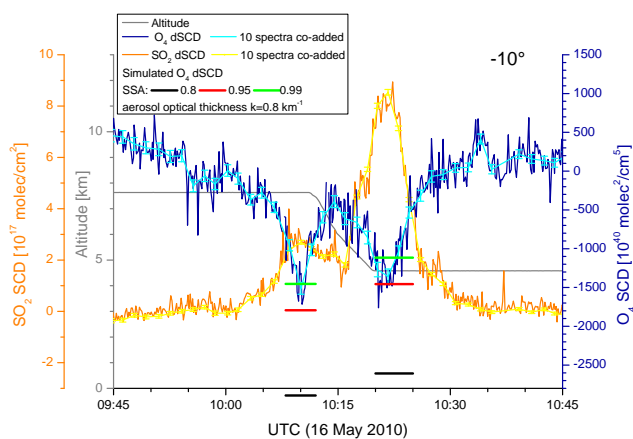


Fig. 6. CARIBIC DOAS O₄ dSCD of the -10° telescope and the flight altitude during the observation of enhanced SO₂ column densities. Also the simulated O₄ dSCD are included for three different values of the Single Scattering Albedo. Due to the volcanic ash the light path through and in the plume is strongly reduced, resulting in lower O₄ slant column densities.

3.3 Other CARIBIC data

As the aeroplane flew over the ash cloud first and went through it after the u-turn, most instruments observed the plume during the second leg. However, just before the first SO₂ peak a small aerosol peak was detected, perhaps remains of an older plume at higher altitude, or a small streak that reached slightly higher. During the flight on 16 May 2010 the optical particle counter (Sec. 2.1) failed. Therefore no information about the size distribution in the range from 125 nm to 1 μ m inside the volcanic ash plume is available. The CPCs (condensation particle counters) measure small particles and cover the size range of 4 nm to 2 μ m providing three size bins of 4–12 nm, 12–18 nm and above 18 nm. The respective results are illustrated in Fig. 8. The first aerosol peak appears not to correlate with DOAS O₄ or SO₂ data. This indicates that the condensation nuclei number density is dominated by small particles, which have only a minor influence on the O₄ SCD. The second and third peak were observed just before the SO₂ column density peak. In contrast to the third peak the aerosol number concentration of the second one reaches background levels before the DOAS instrument observes the plume's maximum. The aerosol data indicate that the aeroplane passed through the main plume during the period when

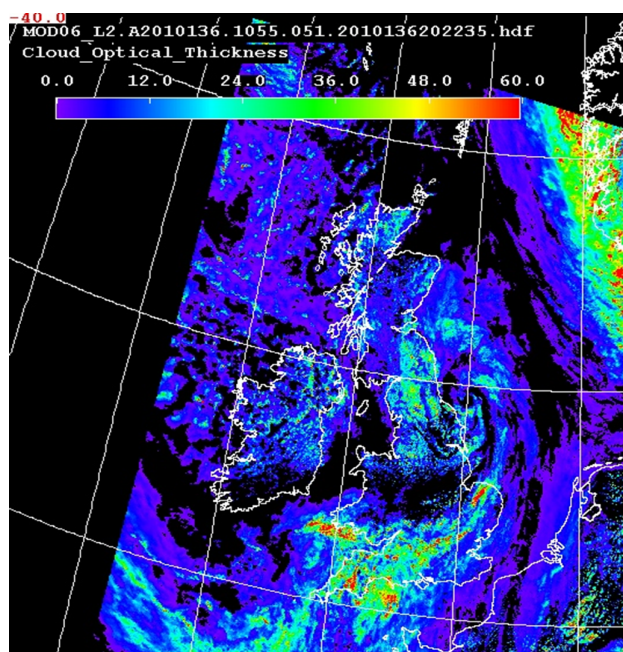


Fig. 7. MODIS cloud optical thickness over the British Isles for 16 May 2010. North of Ireland the COT was around 10 with very small variations.

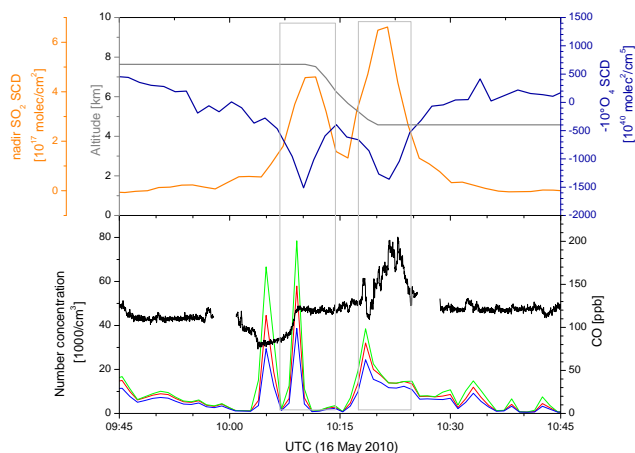


Fig. 8. Overview of some additional CARIBIC observations and the DOAS SO₂ and O₄ data (Fig. 6). Three increases in the aerosol number concentrations occurred. The green, red and blue line corresponds to the size bin above 4 nm, above 12 nm and above 18 nm respectively. The first two peaks are observed at 7600 m, the third one is at a lower flight level (4600 m). The gaps in the CO data are caused by regular automated in-flight-calibration; fortunately the calibrations were performed just before and after crossing the plume.

the second SO₂ peak was observed. Whether or not the first two narrow peaks can be attributed to parts of the plume cannot be inferred from our observation.

Moreover, during the plume observations aerosol samples were collected from 09:59 to 10:49 and 11:38 to 12:27 (Fig. 5). Based on the particle-induced X-ray emission (PIXE) and particle elastic scattering (PESA) analyses the aerosols were clearly identified as being of volcanic origin by their enhanced concentration of several elements such as silicon, potassium, calcium and iron (samples 4 and 6). Hence we found a similar elemental composition as for volcanic ash sample from Iceland Sigmundsson et al. (2010). Flentje et al. (2010) reported a similar composition for rain water probes containing washed out particles at Hohenpeißenberg. In addition to these crustal elements, the CARIBIC aerosol samples contained enhanced concentrations sulphur and carbon, in agreement with observations from the 2008 eruption of the Kasatochi volcano (Martinsson et al., 2009).

During the observation of the second SO₂ peak an increase in CO is observed, while for the first peak a stratospheric signal (a decrease) is found. The increase of 70 ppb is not a specific, but in this case clear indicator for the volcanic plume (e.g. Mori and Notsu, 1997). Schumann et al. (2011) reported lower enhancements (≈ 8 ppb and 13 ppb) for measurements on 16 May and 17 May 2010, respectively in the same region.

These in situ measurements give evidence for volcanic influence during the DOAS observation of the second SO₂ peak. During, or rather prior to the first observation only an increase in aerosol was found, preceding the SO₂ and O₄ column density increase. We conclude that the aeroplane crossed above the plume before it turned around, descended and subsequently crossed the plume. This assumption is also supported by a decrease in some NMHCs (not shown) caused by chlorine chemistry in the plume. Details are given in Baker et al. (2011).

Also mercury and ozone are measured using the CARIBIC flying laboratory. However, in these data no direct evidence of the volcanic plume was found. One would expect a decrease in O₃ caused by the reaction with BrO (Reactions R4 to R6) and an increase in total gaseous mercury due to the volcanic emission. But such effects were not found for the Eyjafjallajökull plumes, discussed here.

3.4 Satellite data

Satellite instruments e.g. OMI (Ozone Monitoring Instrument, Levelt et al., 2006) on EOS-Aura and GOME-2 on MetOp-A (Sect. 2.4) observed the evolution of Eyjafjallajökull's plume right from the beginning (<http://www.Temis.nl>, August 2010). The SO₂ columns were astonishingly low during the first phase of the eruption until 18 April 2010, after which substantial SO₂ column densities were observed. Figure 9 shows the SO₂ and BrO distribution over Western Europe on 16 May 2010. A plume appears to be moving from southern Iceland towards the British Isles, where the remainders of an older plume are located.

The EOS-Aura satellite, carrying also the OMI instrument, passed over Europe around noon (12:51 UTC). To

minimize time differences the CARIBIC data is compared to the GOME-2 data (Fig. 9) where the maximum difference in the overpass times is less than 15 minutes. In Fig. 9 only the forward scans are considered, in the overlap regions (Sect. 2.4) the averages are shown. The SO₂ data show a compact plume situated over northern England, with the BrO plume being patchy. The main reason for the high spatial variation in the BrO is likely to be instrumental noise (Sect. 2.4). For both SO₂ and BrO a slight enhancement is also observed north of Ireland where the CARIBIC flying laboratory observed the plume (6.67° W/56.07° N).

4 Discussion

4.1 CARIBIC DOAS data

Both viewing directions of the DOAS instrument observed the plume twice north of Ireland with the horizontal distance between the two observations being approximately 15 km. Especially in the -10° line of sight the differences between the SO₂ slant column densities are quite obvious (Fig. 5). However, besides variations of the SO₂ concentrations inside the plume also the different sensitivity for the SO₂ layer, caused by the change in flight altitude, is very important for the understanding of the SCDs.

The AMF for SO₂ (315 nm – Fig. 10) and BrO (340 nm) were simulated using the aerosol properties ($k=0.8\text{ km}^{-1}$, SSA=0.95) as retrieved from the O₄ column densities (Sect. 3.2). Inside the plume the visibility is strongly reduced by the volcanic aerosol, therefore the Box AMFs decrease very fast with distance from the aeroplane. To convert the Box-AMF to total AMF the same altitude range as for the aerosol was assumed for BrO and SO₂, i.e. the plume was between 3 and 6 km altitude.

The SO₂ vertical column densities (Eqs. 3 and 4) for -10° and nadir agree quite well (Fig. 11), with only the first observation of the plume with the -10° telescope being slightly smaller than the respective nadir observation. This might be caused by some local variations in the SO₂ concentration, both horizontally and vertically. For BrO this effect is smaller, however as the noise in the -10° data is high, we assume the relative distributions of BrO and SO₂ to be the same. Because the viewing direction changed rapidly during the turn no AMFs are calculated for this part of the flight.

If we assume a constant mixing ratio for the complete layer from 3 to 6 km we retrieve roughly 40 ppb for SO₂ and 5 ppt BrO (Table 3). The values in Table 3 are calculated with the maximum observations of the 80 s averages, the individual 8 seconds spectra result in similar mixing ratios with a $1-\sigma$ variation of 1.8 ppt BrO and 1.2 ppb SO₂ during the observation of the maximum in the nadir data. A better agreement between the vertical columns or the mixing ratios of the four individual observations cannot be expected, since different air masses were observed. The difference of 10 min. corre-

Table 3. Overview of the retrieved BrO and SO₂ mixing ratios based on the CARIBIC DOAS data for the four individual observations of the plume. The variability in the SO₂ data is quite high, which might be caused by the local distribution. Even if the BrO mixing ratio is constant, the error (1.8 ppt) is too high to assume that the distribution differs from the SO₂ distribution.

	BrO [ppt]		SO ₂ [ppb]		$\frac{\text{BrO}}{\text{SO}_2}$ [10 ⁻⁴]	
	-10°	Nadir	-10°	Nadir	-10°	Nadir
1st peak	4.9	4.3	29.3	35.3	1.69	1.22
2nd peak	6.0	4.5	49.7	45.7	1.21	0.98

sponds to a 6 km shift of the plume according to the ruling wind speed (20 knots \approx 10 m/s), which is not enough to compensate for the difference of 15 km between the two observation points. In situ SO₂ measurements on the DLR Falcon over the British east coast reached values over 30 ppb on the same day but a few hours later (Schumann et al., 2011). Considering that a different part of the plume was probed, this is in good agreement with our data.

Depending on the volcano, the BrO to SO₂ ratio is typically in the range between ≈ 0.5 and 10×10^{-4} (e.g. Bobrowski and Platt, 2007). Other important factors are the distance to the crater and the position in the plume (e.g. Bobrowski et al., 2007). At the position of our measurements the ratio is around 1.3×10^{-4} (Fig. 12) and hence well within the typical range. Both the ratio $\frac{\text{VCD}(\text{BrO})}{\text{VCD}(\text{SO}_2)}$ and the linear fit (1st peak: $1.32 \pm 0.16 \times 10^{-4}$; $R^2=0.57$ and 2nd peak: $1.18 \pm 0.09 \times 10^{-4}$; $R^2=0.78$) resulted in lower ratios for the second peak observation. Considering the facts that the total distance to the volcano is about 44 h, that the noise in the BrO data is quite high and that the observed air masses are not the same, this does not contradict the increase in the BrO to SO₂ ratio as predicted and observed by Bobrowski et al. (2007).

In contrast to other observations made close to a volcanic crater (e.g. Bobrowski et al., 2007), we observe no increase in the BrO to SO₂ ratio towards the plume's edges (Fig. 12). This was to be expected as the O₃ mixing ratio in the plume centre (≈ 25 to 50 ppb) is still high enough for the oxidation of bromine (R5). According to von Glasow (2010) between 10 and 30% of the total bromine in the plume is BrO. Consequently the retrieved BrO mixing ratio (Table 3) of 5 ppt therefore results in a total bromine content of 15 to 50 ppt, which is still much lower than the observed ozone mixing ratio of 25–50 ppb.

The horizontal extension of the plume is estimated based on the width of the SO₂ peaks. The fact that two peaks can be distinguished in the time series of the SO₂ and the BrO column densities proves that for the short period in between the aeroplane did neither sample inside the plume nor flew over it. If this short period was due to the fact that the aeroplane

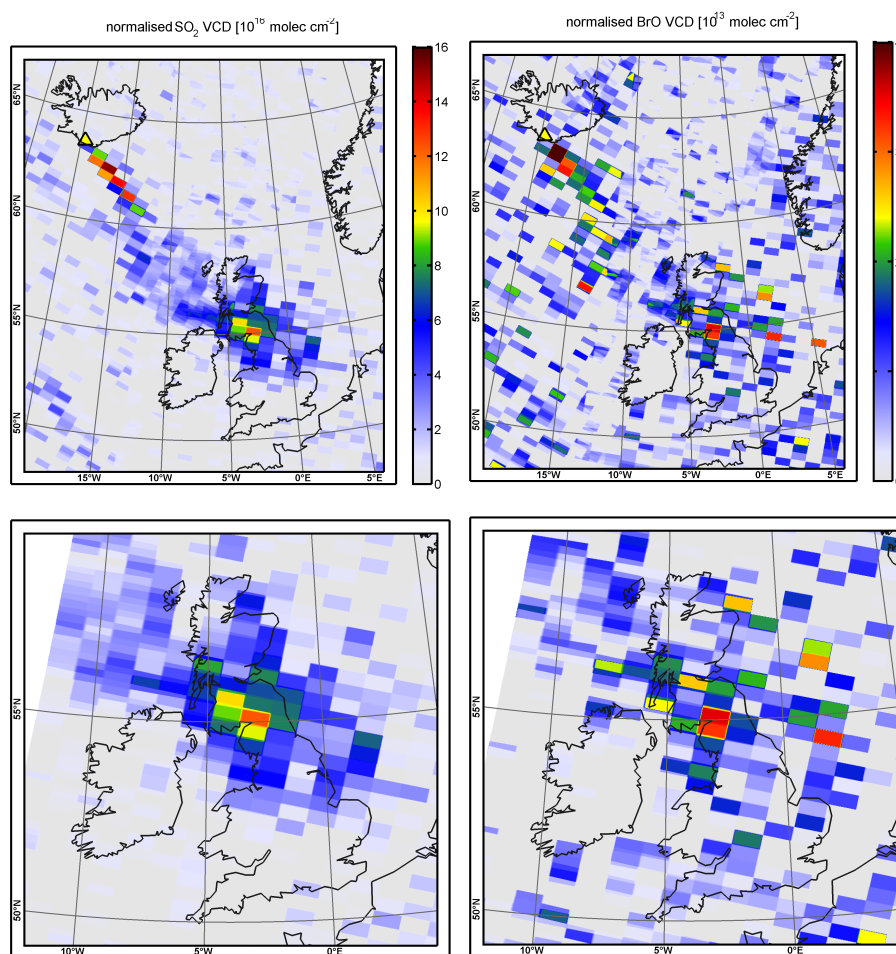


Fig. 9. GOME-2 satellite images showing SO₂ and BrO normalised geometric VCDs (Sec. 2.4) over NW Europe (top) and the British Isles (bottom) on 16 May 2010. For the overview pictures 3 orbits (3 overpasses) are shown and averaged in the overlap regions. The zoom on the British Isles only contains data of one orbit (overpass time 10:09 UTC). There are two major plumes: one is south of Iceland and another one over northern England. The CARIBIC measurements were performed north of Ireland, where a small streak of the plume is found.

briefly left the plume to return later, we calculate that the plume was 60 km wide. Compared to the model prediction (Fig. 3) the observed SO₂ plume is further north and smaller. The fact that the O₄ time series (Fig. 6) show a similar pattern indicates that the SO₂ and the aerosol plume coincide.

4.2 Comparison with GOME-2 satellite data

Comparing airborne DOAS observations with those from satellites always faces two questions:

- What influence has the spatial distribution of the trace gases on the columns observed by the two instruments with different resolution?
- If the spatial variation is small enough, do the instruments agree when the same air masses are observed?

Based on previous comparisons (Heue et al., 2010) we know that both observations can agree very well if the AMFs are calculated using the correct cloud and aerosol description. Therefore for GOME-2 new AMFs were simulated with the same settings (clouds and aerosols) as previously used for CARIBIC (Sect. 3.2). Moreover the datasets have to be corrected for differences in overpass times. In this study the measurements were almost simultaneously i.e. 10:05 to 10:25 UTC for CARIBIC and 10:09 for GOME-2. Therefore large parts of the observed differences are most probably caused by the different spatial resolution of the two instruments in combination with the distribution of the trace gases.

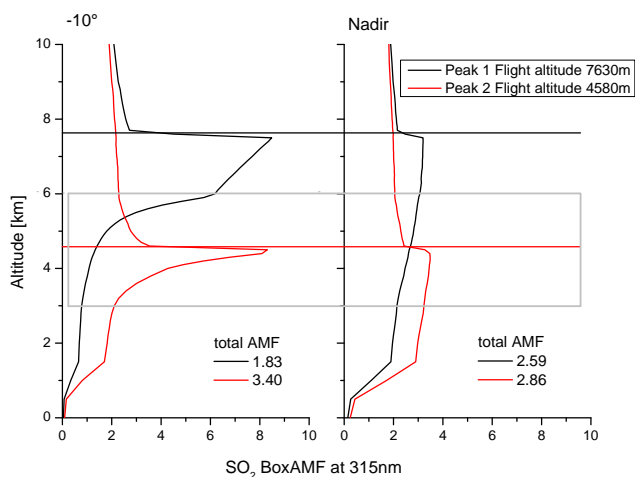


Fig. 10. SO₂ Box AMFs (315 nm) for the viewing geometries used during the plume observations. The horizontal solid lines mark the flight altitude for the respective peak observation. The box covers the estimated plume altitude range (3–6 km). In the simulations a cloud top height of 1.5 km was assumed, which causes the second rapid decrease in the sensitivity below 1.5 km.

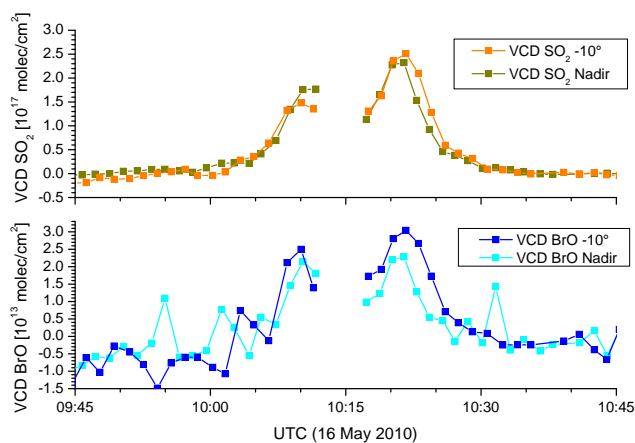


Fig. 11. Vertical column densities for CARIBIC DOAS nadir (brown, light blue) and -10° (orange, dark blue), only the 80 sec averages are shown. The general agreement between the vertical column densities is good.

4.2.1 Sulphur dioxide vertical column densities

A comparison of the SO₂ vertical columns is shown in Fig. 13. Together with the CARIBIC time series, the surrounding GOME-2 pixels are shown for each CARIBIC DOAS observation, including forward and backward scan. All pixels are shown, in case two or three overlap. The lengths of the GOME-2 measurement points in this "time series" are given by the time the CARIBIC system spent in the respective pixel. The figure shows a clear symmetry for GOME-2, which is caused by the fact that before, and after the u-turn CARIBIC flew over the same GOME-2 pixels.

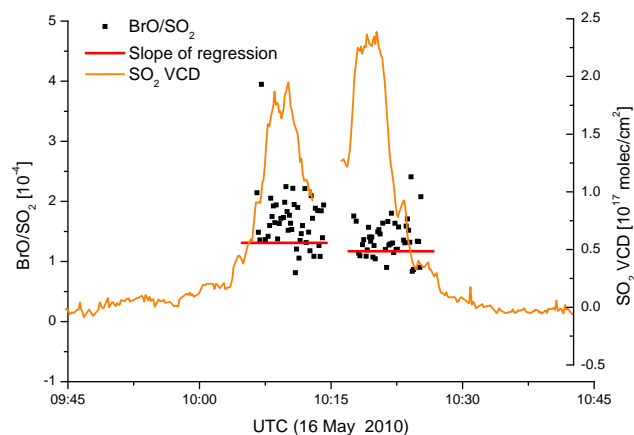


Fig. 12. BrO to SO₂ ratio inside the plume for the CARIBIC nadir data. Beside the BrO to SO₂ ratio the slope of the linear fit for the two observations is shown, $(1.31 \pm 0.16) \times 10^{-4}$ and $(1.17 \pm 0.09) \times 10^{-4}$ for the first and the second peak respectively. The SO₂ vertical column density is also included in the picture.

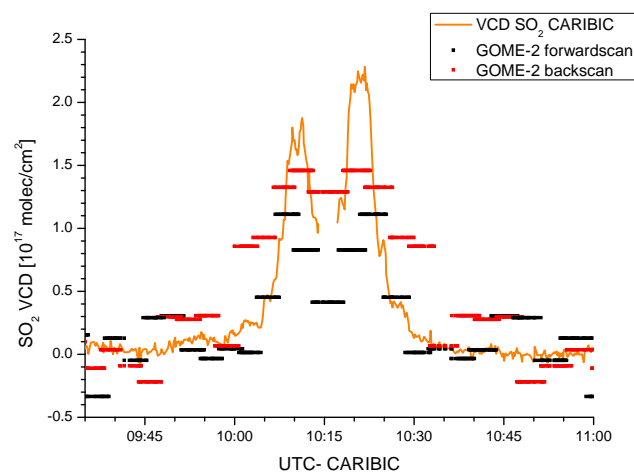


Fig. 13. Comparison of the vertical SO₂ columns, measured by CARIBIC (nadir) and GOME-2. For each CARIBIC DOAS measurement the pixels crossed by the aeroplane (forward and backward scans) are shown. Because the aeroplane made a u-turn just north of the plume, the GOME-2 pixels are the same before and after the turn, resulting in the observed symmetry. During the turn the viewing geometry of CARIBIC changed very rapidly, and therefore no AMFs were calculated here.

The location of the SO₂ maximum agrees well with the CARIBIC observation for both forward and back scan. Also the minimum to the north of the plume (10:15 UTC) can be seen in the GOME-2 dataset. Due to the smaller pixel size the maxima are more pronounced in the forward scan, compared to the back scan, where additional parts of the plume might be observed further east and west. Therefore it is surprising that the better quantitative agreement with respect to

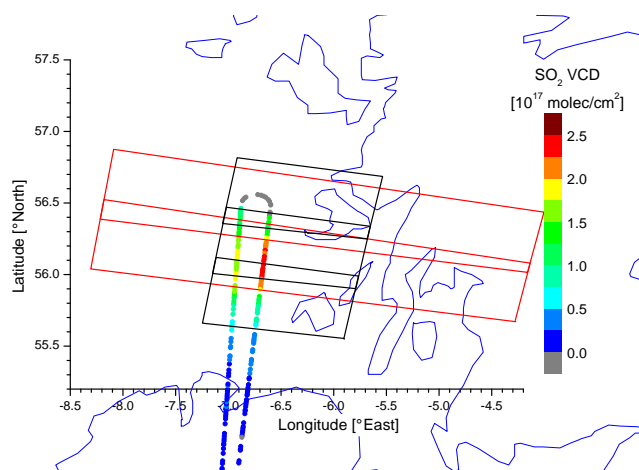


Fig. 14. SO₂ vertical column density from CARIBIC and the observed plume position relative to the GOME-2 pixel (black: forward, red: back scan). In contrast to Figure 2 only those pixels are shown that cover the volcanic plume and at least one measurement from CARIBIC, namely the pixels 21 of swath 26 (North), 27 and 28, as well as the back scan pixel 27 of swath 26 and 27. The maximum of the CARIBIC DOAS SO₂ columns is perfectly covered by one back scan, moreover it is located in the overlapping area of two different forward scan pixels. For the period of the turn no AMF were calculated, therefore the VCD is grey colour coded.

the vertical column density is found for the backward scan. This finding can be understood when taking into account the local distribution of the SO₂ relative to the GOME-2 pixels.

According to Figure 9, the SO₂ plume is almost parallel to the GOME-2 scan direction. If the plume is located in the centre of the back scan, and extends parallel to the pixel orientation, this might explain why the large back scan observes a higher column density than the smaller forward scan. At least at the position of the CARIBIC observation the plume was located in the centre of the back scan (Fig. 14). An alternative explanation for higher back scan columns would be that the maximum is further east or west i.e. there is a second SO₂ maximum covered by the back scan but not observed by the respective forward scan. This implies that it is observed by any other forward scan overlapping with this back scan.

The vertical column density for the back scan (swath 27) is 1.49×10^{17} molec/cm², the VCDs for the respective forward scans are listed in Table 4. Only pixel 19 of swath 28 (not shown in Fig. 2) has a VCD that is higher than the backward scan, due to its small overlap (≈ 390 km²) it contributes less than 4% to the back scan VCD.

80% of the area of the forward pixel 21 (swath 27) is also covered by the back scan. Therefore the contribution of the back scan signal to this forward scan can easily be estimated. If the plume was homogeneously distributed inside the back scan, then the signal of this forward pixel would be higher than 1.2×10^{17} molec/cm², even if the VCD vanished in the other 20% of the pixel. Therefore the SO₂ column den-

Table 4. Vertical SO₂ column densities in 10^{17} molec/cm² for the GOME-2 forward scan pixels overlapping with that back scan where the maximum of 1.49×10^{17} molec/cm² in SO₂ is observed. In black are those pixels that are also probed by CARIBIC and in grey are the neighbouring pixels.

PixelNo	19	20	21	22	27 back scan (swath 27)
SwathNo					
27	1.12	1.25	0.86	0.37	
28	1.86	1.28	1.14	1.43	1.49

sity cannot have been homogeneously distributed in the back scan. Of course this was not to be expected, especially as the CARIBIC data already showed the local variability.

A combination of the CARIBIC and GOME-2 data might be used to estimate the size of the part of the plume which was observed by CARIBIC. The plume is about 60 km wide (Fig. 14) and the distance between the two CARIBIC observations is about 15 km. If we assume this part of the plume to be 60×40 km² with an average VCD of 2×10^{17} molec/cm² (Fig. 14) then it contributes about 98% to the column density observed by GOME-2 forward scan (pixel 21 of swath 27), and 49% to the VCD of the pixel 21 of swath 28. The assumption that the plume expands over 80 km i.e. that it stretches over the complete pixel results in a VCD of 1.7×10^{17} molec/cm² and hence contradicts the observed VCD for pixel 21, swath 27. The same assumption however might explain about 98% of the observed VCD of the same pixel in the next swath (28). The plume was weighted with 75% and 50% as it is not completely covered by the pixel 21 of swath 27 and 28 respectively.

Hence the local variability of the SO₂ concentration or vertical column density must have been higher than expected from CARIBIC and the GOME-2 observations. In this estimate we assumed that outside the plume the vertical column vanishes, but even with this simple approximation we partly overestimated the GOME-2 signal.

To conclude, the plume we observed here with CARIBIC and GOME-2 was about 60 km wide. For the northern GOME-2 pixel 21 (swath 27) the length inside the pixel was roughly 30 km or slightly more. For the southern pixel 21 (swath 28) the estimated length is close to 80 km (covering the entire length of the pixel). Hence locally the plume did not extend parallel to the GOME-2 pixels but turns south. The shift according to the wind and time is insignificant, since 12 km to the west (15 min) is not enough to transport the observed part of the plume to a different GOME-2 pixel (Fig. 14).

4.2.2 Bromine monoxide vertical column densities

In the CARIBIC DOAS observations SO₂ and BrO do coincide (Fig. 5), indicating that the position of the maxima in

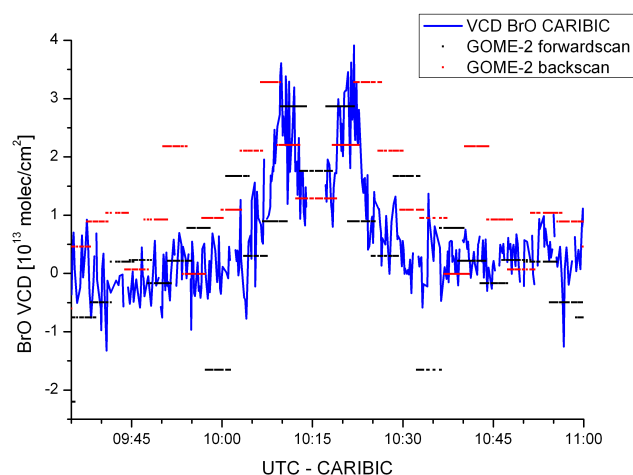


Fig. 15. Comparison of the BrO vertical column densities. Again the structure of the BrO peaks is well discernible in the GOME-2 data and also the vertical column densities are very similar.

the plume are the same. In contrast the BrO maxima in the GOME-2 data are shifted north compared to SO₂ (Fig. 9). Despite this spatial shift in the GOME-2 BrO data, the BrO VCDs of CARIBIC and GOME-2 agree quite well (Fig. 15). Compared to SO₂ (Fig. 14) both data sets are noisier, therefore a detailed study of the local distribution including forward and back scan as well as CARIBIC data cannot be accurate. Nevertheless one interesting case shall be mentioned: at the southern edge of the plume (10:08 and 10:24 UTC) the forward scan observes the background level, whereas the overlapping back scan agrees quite well with maximum of the CARIBIC DOAS measurement. But this agreement is likely caused by higher BrO values observed further east (Fig. 9, at 5° W, over the British coast).

As both BrO and SO₂ observations for CARIBIC DOAS and GOME-2 agree well, also the BrO to SO₂ ratio at this position should be similar. However, as the BrO data are close to the detection limit, the calculated ratio of the VCDs inside the plume varies between -0.2 and 2.8×10^{-4} . The linear regression of the plot BrO over SO₂ for the GOME-2 in the area of the CARIBIC measurements (swath 26–30, Pixel 20–22+27, Table 4) has a slope of $(1.3 \pm 0.56) \times 10^{-4}$ with a correlation of $R^2 = 0.16$. This demonstrates that BrO to SO₂ ratio can only be calculated when both column densities are well above the detection limit. For future satellite studies on this topic larger areas and higher column densities should be used.

5 Conclusions

The Eyjafjallajökull plume was observed by several instruments of the CARIBIC flying observatory during the special volcanic mission flight on 16 May 2010. While the re-

mote sensing DOAS instrument observed the plume twice north of Ireland, many in situ instruments observed the plume only in the second case. This shows that the aeroplane first flew over the plume, turned around to subsequently cross it. Moreover, it highlights the importance of the remote sensing aspect of the DOAS instrument as a part of CARIBIC. Additional information from the aerosol counters and carbon monoxide instrument is used to determine whether or not the aeroplane was inside the plume, because this is essential for the description of the atmosphere during the AMF calculation. Unfortunately the optical particle counter, which would have given useful additional information on the aerosol size distribution failed during this flight. Chemical confirmation that the observed plume originated from the Eyjafjallajökull volcano was given by comparing elemental composition of collected aerosol samples with that reported for volcanic ash from Iceland. The video camera was for the first time in the CARIBIC project used to give a rough approximation of the cloud top height, which is however limited by the coarse resolution of the video images.

Based on the O₄ column density, the aerosol extinction and single scattering albedo were retrieved. Compared to MODIS satellite data, the retrieved total aerosol optical depth is higher by a factor of 2. The retrieved information was used to calculate the local SO₂ and BrO mixing ratios inside the plume to 40 ppb (29–49) and 5 ppt (4.3–6.0), respectively. The observed BrO to SO₂ ratio of 1.3×10^{-4} (0.9–1.6) is well within the range typically observed at other volcanoes. The SO₂ mixing ratio agrees well with in situ observation from the DLR Falcon further east. For the small part of the plume sampled during this flight, the MetOffice dispersion model predicted the plume further south and wider than it actually was.

A good agreement is observed between GOME-2 and CARIBIC DOAS for the sulphur dioxide vertical columns, provided the cloud altitude and the aerosol extinction in the plume are considered in the AMF calculation. The GOME-2 BrO columns are close to the detection limit, however, a reasonable agreement was observed here as well. A more detailed study on the column densities observed by the GOME-2 forward scan and the back scan showed that the local variability of SO₂ concentration is very high. By combining the CARIBIC and the GOME-2 vertical columns we estimated that the observed part plume was 60 km wide and did not cover the entire length (80 km) of the GOME-2 pixels. While the length of the plume in the northern pixel was roughly 30 to 40 km, in the southern part the length almost reached the length of the whole pixel. The BrO to SO₂ ratio could not be calculated for the GOME-2 data in the area around the CARIBIC observation, as the measurement noise for the BrO data was too high. So for future satellite studies we recommend to use larger parts of the plume.

Acknowledgements. For providing the MODIS data at <http://ladsweb.nascom.nasa.gov/> the MODIS team is acknowledged. The volcanic ash forecast groups especially at MetOffice are acknowledged for the forecasts used during flight preparation. Also Ulrich Schumann and the DLR Falcon scientific group are acknowledged for sharing some experiences and preliminary results. We thank Lufthansa Airlines for giving us the opportunity to measure under these unique conditions especially Captain Martin Hoell, Andreas Waibel, Thomas Dauer, Sven Dankert and Detlev Hartwig and of course the CARIBIC Team for their commitment and support. The DOAS system was built and operated by the Institut für Umweltphysik of the Universität Heidelberg. Rinus Scheele (KNMI) is acknowledged for helping with the trajectory calculations. The development and operation of the CARIBIC system has been financially supported by the German Bundesministerium für Bildung und Forschung (BMBF-AFO 2000), by the European Commission's DGXII Environment RTD 4th, 5th and 6th framework programs, by the Max-Planck-Society, EON-Ruhrgas and Frankfurt Airport.

The service charges for this open access publication have been covered by the Max-Planck-Society.

Edited by: W. Birmili

References

- Ansmann, A., Tesche, M., Groß, S., Freudenthaler, V., Seifert, P., Hiesch, A., Schmidt, J., Wandinger, U., Mattis, I., Müller, D., and Wiegner, M.: The 16 April 2010 major volcanic ash plume over central Europe: EARLINET lidar and AERONET photometer observations at Leipzig and Munich, Germany, *Geophys. Res. Lett.*, 37, L13810, doi:10.1029/2010GL043809, 2010.
- Baker, A. K., Schuck, T. J., Slemr, F., van Velthoven, P., Zahn, A., and Brenninkmeijer, C. A. M.: Characterization of non-methane hydrocarbons in Asian summer monsoon outflow observed by the CARIBIC aircraft, *Atmos. Chem. Phys.*, 11, 503–518, doi:10.5194/acp-11-503-2011, 2011.
- Baker, A. K., Rauthe-Schöch, A., Schuck, T. J., Brenninkmeijer, C. A. M., van Velthoven, P. F. J., Wisher, A. and Oram, D. E.: Investigation of chlorine radical chemistry in the Eyjafjallajökull volcanic plume using observed depletions in non-methane hydrocarbons, *Geophys. Res. Lett.*, submitted, 2011.
- Bani, P., Oppenheimer, C., Tsanev, V. I., Carn, S. A., Cronin, S. J., Crimp, R., Calkins, J. A., Charley, D., Lardy, M., Roberts, T. R.: Surge in sulphur and halogen degassing from Ambrym volcano, Vanuatu, *Bull. Volcanol.*, 71, 1159–1168, doi:10.1007/s00445-009-0293-7, 2009.
- Bobrowski, N. and Platt, U.: SO₂/BrO ratios studied in five volcanic plumes, *J. Volcanol. Geotherm. Res.* 166, 147–160, doi:10.1016/j.jvolgeores.2007.07.003, 2007.
- Bobrowski, N., Hönninger, G., Galle, B., and Platt, U.: Detection of bromine monoxide in a volcanic plume, *Nature*, 423, 273–276, doi:10.1038/nature01625, 2003.
- Bobrowski, N., Glasow, R. von, Aiuppa, A., Inguaggiato, S., Louban, I., Ibrahim, O. W., and Platt, U.: Reactive halogen chemistry in volcanic plumes, *J. Geophys. Res.*, 112, D06311, doi:10.1029/2006JD007206, 2007.
- Bogumil, K., Orphal, J., Homann, T., Voigt, S., Spietz, P., Fleischmann, O. C., Vogel, A., Hartmann, M., Bovensmann, H., Frerik, J., and Burrows, J. P.: Measurements of Molecular Absorption Spectra with the SCIAMACHY Pre-Flight Model: Instrument Characterization and Reference Data for Atmospheric Remote-Sensing in the 230–2380 nm Region, *J. Photochem. Photobiol. A-Chem.*, 157, 167–184, doi:10.1016/s1010-6030(03)00062-5, 2003.
- Brenninkmeijer, C. A. M., Crutzen, P., Boumard, F., Dauer, T., Dix, B., Ebinghaus, R., Filippi, D., Fischer, H., Franke, H., Frieß, U., Heintzenberg, J., Helleis, F., Hermann, M., Kock, H. H., Koepfel, C., Lelieveld, J., Leuenberger, M., Martinsson, B. G., Miemczyk, S., Moret, H. P., Nguyen, H. N., Nyfeler, P., Oram, D., O'Sullivan, D., Penkett, S., Platt, U., Pupek, M., Ramonet, M., Randa, B., Reichelt, M., Rhee, T. S., Rohwer, J., Rosenfeld, K., Scharffe, D., Schlager, H., Schumann, U., Slemr, F., Sprung, D., Stock, P., Thaler, R., Valentino, F., van Velthoven, P., Waibel, A., Wandel, A., Waschitschek, K., Wiedensohler, A., Xueref-Remy, I., Zahn, A., Zech, U., and Ziereis, H.: Civil Aircraft for the regular investigation of the atmosphere based on an instrumented container: The new CARIBIC system, *Atmos. Chem. Phys.*, 7, 4953–4976, doi:10.5194/acp-7-4953-2007, 2007.
- Bussemer, M.: Der Ring-Effekt: Ursachen und Einfluß auf die Messung stratosphärischer Spurenstoffe, diploma thesis, Univ. of Heidelberg, Germany 1993.
- Carn S. A., Krueger, A. J., Krotkov, N. A., Yang, K., and Evans, K.: Tracking volcanic sulfur dioxide clouds for aviation hazard mitigation, *Nat. Hazards*, 51, 325–343, doi:10.1007/s11069-008-9228-4, 2009.
- Deutschmann, T.: Atmospheric Radiative Transfer Modelling with Monte Carlo Methods, diploma thesis Univ. of Heidelberg, Germany, 2009.
- Dix, B., Brenninkmeijer, C. A. M., Frieß, U., Wagner, T., and Platt, U.: Airborne multi-axis DOAS measurements of atmospheric trace gases on CARIBIC long-distance flights, *Atmos. Meas. Tech.*, 2, 639–652, doi:10.5194/amt-2-639-2009, 2009.
- Dyroff, C., Fütterer, D., and Zahn, A.: Compact diode-laser spectrometer ISOWAT for highly sensitive airborne measurements of water-isotope ratios. *Applied Physics B-Lasers and Optics* 98(2-3), 537–548, doi:10.1007/s00340-009-3775-6, 2010.
- Flentje, H. and Claude, H. and Elste, T. and Gilge, S. and Köhler, U. and Plass-Dülmer, C. and Steinbrecht, W. and Thomas, W. and Werner, A. and Fricke, W.: The Eyjafjallajökull eruption in April 2010 – detection of volcanic plume using in-situ measurements, ozone sondes and lidar-ceilometer profiles, *Atmos. Chem. Phys.*, 10, 10085–10092, doi:10.5194/acp-10-10085-2010, 2010.
- Frieß, U., Monks, P. S., Remedios, J. J., Rozanov, A., Sinreich, R., Wagner, T., and Platt, U.: MAX-DOAS O₄ measurements: A new technique to derive information on atmospheric aerosols: 2. Modelling studies, *J. Geophys. Res.*, 111, D14203, doi:10.1029/2005JD006618, 2006.
- Grainger, J. and Ring, J.: Anomalous Fraunhofer line profiles, *Nature*, 193, 762, doi:10.1038/193762a0, 1962.
- Greenblatt, G. D., Orlando, J. J., Burkholder, J. B., and Ravishankara, A. R.: Absorption measurements of oxygen between 330 and 1140 nm, *J. Geophys. Res.*, 95, 18577–18582, doi:10.1029/JD095iD11p18577, 1990.
- Gür, B., Spietz, P., Orphal, J., and Burrows, J.: Absorption Spectra Measurements with the GOME-2 FMs using the IUP/IFE-UBS

- Calibration Apparatus for Trace Gas Absorption Spectroscopy CATGAS, Final Report, IUP University of Bremen, Germany, 2005.
- Heue, K.-P.: Airborne Multi AXes DOAS instrument and measurements of two dimensional trace gas distribution, Ph.D. thesis, Univ. of Heidelberg, Germany, 2005.
- Heue, K.-P., Brenninkmeijer, C. A. M., Wagner, T., Mies, K., Dix, B., Frieß, U., Martinsson, B. G., Slemr, F. and van Velthoven P. F. J.: Observations of the 2008 Kasatochi volcanic SO₂ plume by CARIBIC aircraft DOAS and the GOME-2 satellite. *Atmos. Chem. Phys.*, 10, 4699–4713, doi:10.5194/acp-10-4699-2010, 2010.
- Kattner, L., Dyroff, C. and Zahn, A.: An ICOS laser spectrometer for regular in-situ measurements of CH₄ and CO₂ aboard the CARIBIC passenger aircraft, Poster presentation at EGU general Assembly, Vienna (2–7 May) EGU2010-9997, 2010.
- Kromminga, H., J. Orphal, J., Spietz, P., Voigt, S. and Burrows, J. P.: New measurements of OClO absorption cross sections in the 325–435 nm and their temperature dependence between 213–293 K, *J. Photochem. Photobiol. A: Photochem.*, 157, 149–160, doi:10.1016/s1010-6030(03)00071-6, 2003.
- Levelt, P. F., van den Oord, G. H. J., Dobber, M. R., Mälkki, A., Visser, H., de Vries, J., Stammes, P., Lundell, J., and Saari, H.: The Ozone Monitoring Instrument, *IEEE Trans. Geo. Rem. Sens.*, 44, 5, 1093–1101, doi:10.1109/TGRS.2006.872333, 2006.
- Martinsson, B. G., Brenninkmeijer, C. A. M., Carn, S. A., Hermann, M., Heue, K.-P., van Velthoven, P. F. J., and Zahn, A.: Influence of the 2008 Kasatochi volcanic eruption on sulfurous and carbonaceous aerosol constituents in the lower stratosphere, *Geophys. Res. Lett.*, 36, L12813, doi:10.1029/2009GL038735, 2009.
- Meller, R. and Moortgat, G., K.: Temperature dependence of the absorption cross sections of formaldehyde between 223 and 323 K in the wavelength range 225–375 nm, *J. Geophys. Res.*, 201(D6), 7089–7101, 2000.
- Mori, T. and Notsu, K.: Remote CO, COS, CO₂, SO₂, HCl detection and temperature estimation of volcanic gas, *Geophys. Res. Lett.*, 24, 2047–2050, doi:10.1029/97GL52058, 1997.
- Nguyen, H. N., Gudmundsson, A., and Martinsson, B. G.: Design and calibration of a multi-channel aerosol sampler for tropopause region studies from the CARIBIC platform, *Aerosol Sci. Tech.*, 40, 649–655, doi:10.1080/02786820600767807, 2006.
- Platt, U. and Stutz, J.: *Differential Optical Absorption Spectroscopy, Principles and Applications*, Springer Berlin Heidelberg, Germany, 2008.
- Pukite, J., Kühl, S., Deutschmann, T., Platt, U., and Wagner, T.: Extending differential optical absorption spectroscopy for limb measurements in the UV, *Atmos. Meas. Tech.*, 3, 631–653, doi:10.5194/amt-3-631-2010, 2010.
- Richter, A., Wittrock, F., Schönhardt, A., and Burrows, J. P.: Quantifying volcanic SO₂ emissions using GOME-2 measurements, Poster presentation: EGU General Assembly, Vienna, Austria, AS3.15 XY247, available at: http://www.iup.uni-bremen.de/doas/posters/egu_2009_richter.pdf, last access: 11 January 2010, 19–24 April 2009.
- Sander, R., Vogt, R., Harris, G. W. and Crutzen, P. J.: Modeling the chemistry of ozone, halogen compounds and hydrocarbons in the arctic troposphere during spring, *Tellus 49B*, 5, 522–532, 1997.
- Scheele, M. P., Siegmund, P. C., and van Velthoven, P. F. J.: Sensitivity of trajectories to data resolution and its dependence on the starting point: in or outside a tropopause fold, *Meteorol. Appl.*, 3, 267–273, 1996.
- Schuck, T. J., Brenninkmeijer, C. A. M., Slemr, F., Xueref-Remy, I., and Zahn, A.: Greenhouse gas analysis of air samples collected on board the CARIBIC passenger aircraft, *Atmos. Meas. Tech.*, 2, 449–464, doi:10.5194/amt-2-449-2009, 2009.
- Schumann, U., Weinzierl, B., Reitebuch, O., Schlager, H., Minikin, A., Forster, C., Baumann, R., Sailer, T., Graf, K., Mannstein, H., Voigt, C., Rahm, S., Simmet, R., Scheibe, M., Lichtenstern, M., Stock, P., Rba, H., Schuble, D., Tafferner, A., Rautenhaus, M., Gerz, T., Ziereis, H., Krautstrunk, M., Mallaun, C., Gayet, J.-F., Lieke, K., Kandler, K., Ebert, M., Weinbruch, S., Stohl, A., Gasteiger, J., Groß, S., Freudenthaler, V., Wiegner, M., Ansmann, A., Tesche, M., Olafsson, H., and Sturm, K.: Airborne observations of the Eyjafjalla volcano ash cloud over Europe during air space closure in April and May 2010, *Atmos. Chem. Phys.*, 11, 2245–2279, doi:10.5194/acp-11-2245-2011, 2011.
- Sigmundsson, F., Hreinsdottir, S., Hooper, A., Arnadottir, T., Pedersen, R., Roberts, M. J., Oskarsson, N., Auriac, A., Decriem, J., Einarsson, P., Geirsson, H., Hensch, M., Ofeigsson, B. G., Sturkell, E., Sveinbjornsson, H. and Feigl, K. L.: Intrusion triggering of the 2010 Eyjafjallajökull explosive eruption, *Nature*, 468, 426–U253, doi:10.1038/nature09558, 2010.
- Simpson, W. R., von Glasow, R., Riedel, K., Anderson, P., Ariya, P., Bottenheim, J., Burrows, J., Carpenter, L. J., Frieß, U., Goodsite, M. E., Heard, D., Hutterli, M., Jacobi, H.-W., Kaleschke, L., Neff, B., Plane, J., Platt, U., Richter, A., Roscoe, H., Sander, R., Shepson, P., Sodeau, J., Steffen, A., Wagner, T., and Wolff, E.: Halogens and their role in polar boundary-layer ozone depletion, *Atmos. Chem. Phys.*, 7, 4375–4418, doi:10.5194/acp-7-4375-2007, 2007.
- Stohl, A., Haimberger, L., Scheele, M. P., and Wernli, H.: An intercomparison of results from three trajectory models, *Meteorol. Appl.*, 8, 127–135, 2001.
- Theys, N., van Roozendaal, M., Dils, B., Hendrick, F., Hao, N., and De Maziere, M.: First satellite detection of volcanic bromine monoxide emission after the Kasatochi eruption, *Geophys. Res. Lett.*, 36, L03809, doi:10.1029/2008GL036552, 2009.
- Vandaele, A. C., Hermans, C., Simon, P., C., van Roozendaal, M., Guilmot, J. M., Carleer, M., Colin, R.: Fourier transform measurement of NO₂ absorption cross section in the visible range at room temperature, *J. Atmos. Chem.* 25(3), 289–305, 1996.
- van Roozendaal, M., Loyola, D., Spurr, R., Balis, D., Lambert, J.-C., Livschitz, Y., Valks, P., Ruppert, T., Kenter, P., Fayt, C., and Zehner, C.: Ten years of GOME/ERS-2 total ozone data-The new GOME data processor (GDP) version 4: 1. Algorithm description, *J. Geophys. Res.*, 111, D14311, doi:10.1029/2005JD006375, 2006.
- von Glasow, R.: Atmospheric chemistry in volcanic plumes, *PNAS*, 107(15), 6594–6599, doi:10.1073/pnas.0913164107, 2010.
- von Glasow, R., Bobrowski, N., Kern, C.: The effects of volcanic eruptions on atmospheric chemistry, *Chemical Geology* 263, 131–142, doi:10.1016/j.chemgeo.2008.08.020, 2009.
- Wagner, T., Dix, B., von Friedeburg, C., Frieß, U., Sanghavi, S., Sinreich, R., and Platt, U.: MAX-DOAS O₄ measurements: A new technique to derive information on atmospheric aerosols – Principles and information content, *J. Geophys. Res.*, 109,

- D22205, doi:10.1029/2004JD004904, 2004.
- Wagner, T., Beirle, S., and Deutschmann, T.: Three-dimensional simulation of the Ring effect in observations of scattered sun light using Monte Carlo radiative transfer models, *Atmos. Meas. Tech.*, 2, 113–124, doi:10.5194/amt-2-113-2009, 2009.
- Wilmouth, D. M., Hanisco, T. F., Donahue, N. M., and Anderson, J. G.: Fourier transform ultraviolet spectroscopy of the A 2Π_{3/2} ← X 2Π_{3/2} transition of BrO, *J. Phys. Chem. A*, 103, 8935–8945, 1999.
- Yang, K., Krotkov, N. A., Krueger, A. J., Carn, S. A., Bhartia, P. K., and Levelt, P. F.: Improving retrieval of volcanic sulfur dioxide from backscattered UV satellite observations, *Geophys. Res. Lett.*, 36, L03102, doi:10.1029/2008GL036036, 2009.